

High-temperature Superconductivity in Perovskite Hydride below 10 GPa

Mingyang Du¹, Hongyu Huang¹, Zihan Zhang², Min Wang¹, Hao Song^{1,*}, Defang Duan², Tian Cui^{1,2,*}

¹ Institute of High Pressure Physics, School of Physical Science and Technology, Ningbo University, Ningbo, 315211, People's Republic of China

² College of Physics, Jilin University, Changchun 130012, People's Republic of China

KEYWORDS: Hydrides, High pressure, Superconductivity, First principles calculation.

*Correspondence authors. songhao@nbu.edu.cn, cuitian@nbu.edu.cn

ABSTRACT

Hydrogen and hydrides materials have long been considered promising materials for high-temperature superconductivity. But the extreme pressures required for the metallization of hydrogen-based superconductors limit their applications. Here, we have designed a series of high-temperature perovskite hydrides that can be stable within 10 GPa. Our research covered 182 ternary systems and ultimately determined that 9 compounds were stable within 20 GPa, of which 5 exhibited superconducting transition temperatures exceeding 120 K within 10 GPa. Excitingly, KGaH_3 and CsInH_3 are thermodynamically stable at 50 GPa. Among these perovskite hydrides, alkali metals are responsible for providing a fixed amount of charge and maintaining structural stability, while the cubic framework formed by IIIA group elements and hydrogen is crucial for high-temperature superconductivity. This work will inspire further experimental exploration and take an important step in the exploration of low-pressure stable high-temperature superconductors.

Introduction

The discovery of superconductors with high transition temperatures (T_c) has been a long-standing hot topic in the scientific community. Since the discovery of superconductivity of mercury in 1911, room-temperature superconductivity has been a long-sought dream and a field of intensive research. In 1935, E. Wigner and H. B. Huntington theoretically predicted that solid metal hydrogen can be obtained under high pressure conditions¹. According to the BCS theory, the superconducting transition temperature of material is proportional to its Debye temperature². This suggests that hydrogen, the lightest element in nature, would be an ideal room-temperature superconductor after metallization³. However, experimental studies have shown that hydrogen requires extremely high pressures to metallize^{4, 5}. As a result, the search for room-temperature superconductor has gradually turned to another, more feasible route — hydrogen-rich compounds.

By incorporating other elements to create a "chemical pre-compression" effect on hydrogen, hydrogen-rich compounds can metallize at much lower pressures than pure hydrogen⁶. Guided by this principle, many excellent hydrogen-rich compounds have been designed and predicted to be potential high-temperature superconductors in the past decade⁷⁻⁹, some of which have been experimentally confirmed. In particular, H_3S and LaH_{10} were first predicted to have superconducting transition temperatures (T_c s) exceeding 200 K¹⁰⁻¹², which have been confirmed experimentally¹³⁻¹⁶. These are important milestones in the exploration of hydrogen-based superconductors.

Among these hydrogen-based superconductors, clathrate superhydrides have attracted extensive attention due to their outstanding superconductivity. They are widely found in alkaline

earth metals and rare earth element superhydrides RH_n ($n = 6, 9, 10$), such as binary hydrides CaH_6^{17} , MgH_6^{18} , $YH_{6,9,10}^{11, 12, 19}$, ScH_6^{20} , $(Tm/Yb/Lu)H_6^{21}$, and ternary hydrides $(Y,Ca)H_6^{22-24}$, $(Mg,Ca)H_6^{25}$, $(Sc,Ca)H_6^{26}$, $(La,Y)H_6^{27}$, $(Ca/Sc/Y,Yb/Lu)H_6^{28}$. In the structure of these superhydrides, H atoms are weakly covalently bonded each other to form H_{24} , H_{29} and H_{32} cage, and the metal atom is located in the center of the H cage. After LaH_{10} confirmed the great potential of clathrate superhydrides in high-temperature superconductivity, more clathrate superhydrides were experimentally synthesized, including ThH_9^{29} , ThH_{10}^{29} , YH_9^{30-32} , $CaH_6^{33, 34}$, YH_6^{35} , CeH_9^{36} , $(La,Y)H_{10}^{37}$, $(La,Ce)H_{9,10}^{38, 39}$.

In this work, we have designed a series of high-temperature superconductors that can be stable within 10 GPa based on perovskite structure of $Pm-3m-KInH_3^{40}$. Our research covered 182 ternary systems and ultimately determined that 9 compounds were stable within 20 GPa, of which 5 exhibited superconducting transition temperatures exceeding 120 K within 10 GPa. Excitingly, $KGaH_3$ and $CsInH_3$ are thermodynamically stable at 50 GPa. Among these perovskite hydrides, alkali metals are responsible for providing a fixed amount of charge and maintaining structural stability, while the cubic framework formed by IIIA group elements and hydrogen is crucial for high-temperature superconductivity. This work will inspire further experimental exploration and take an important step in the exploration of low-pressure stable high-temperature superconductors.

Computational details

Ab initio random structure searching (AIRSS) technique^{41, 42} and ab initio calculation of the Cambridge Serial Total Energy Package (CASTEP)⁴³ were used to predict the candidate crystal

structures of AXH₃. The generalized gradient approximation with the Perdew-Burke-Ernzerhof parametrization⁴⁴ for the exchange-correlation functional and on-the-fly generation of ultra-soft potentials were used for the structure searching.

The Vienna ab initio simulation program (VASP)⁴⁵ was used for structural relaxation and calculations of enthalpies and electronic properties. The projector augmented plane-wave potentials⁴⁶ with an energy cutoff of 800 eV and Monkhorst-Pack⁴⁷ meshes for Brillouin zone sampling with resolutions of $2\pi \times 0.03 \text{ \AA}^{-1}$ were used to ensure that all enthalpy calculations are well converged to less than 1 meV per atom.

The Quantum-ESPRESSO⁴⁸ was used in phonon and electron-phonon calculations. Ultra-soft potentials were used with a kinetic energy cut-off of 90 Ry. The k-points and q-points meshes in the first Brillouin zone are $12 \times 12 \times 12$ and $6 \times 6 \times 6$. The superconducting transition temperatures of these structures are estimated through the self-consistent iteration solution of the Eliashberg equation (scE)⁴⁹.

Results and discussion

Using the perovskite structure of *Pm-3m*-KInH₃ as a template, we obtained a series of compounds AXH₃ by substituting the IA-IVA elements and IIB elements, with the structure shown at the middle of Fig. 1. The A indicates Alkali metals, alkaline earth metals, rare earth metals, and the X indicates IIIA or IVA elements. All the elements involved in this study are shown in Fig. 1.

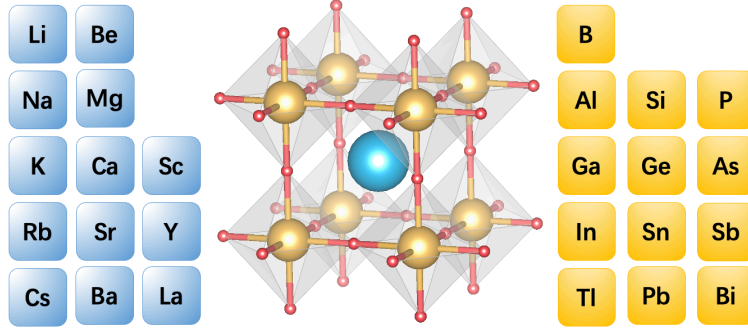


Fig. 1. Crystal structure of the perovskite hydrides AXH_3 . Blue, yellow, and red balls represent A (group IA, IIA or IIIB metal), X (group IIIA, IVA or VB element), and H atoms, respectively.

We first did a screening for the dynamical stability of perovskite hydrides AXH_3 with space group $Pm-3m$ at 0-50 GPa. The Quantum-ESPRESSO code was used to initially verify the dynamical stability of these compounds. In this study, we have uncovered nine dynamically stable perovskite hydrides, $KAlH_3$, $RbAlH_3$, $KGaH_3$, $RbGaH_3$, $KInH_3$, $RbInH_3$, $CsInH_3$, $RbTlH_3$, $CsTlH_3$, which are marked by circles in Fig. 2. The gray cross indicates that this structure cannot be stable within 50 GPa. Perhaps these structures can remain stable under higher pressures, but it is unlikely that these perovskite hydrides have T_c exceeding 200 K, at pressures exceeding 50 GPa, they do not have significant advantages compared to other high-temperature superconducting materials. Therefore, in this work, we will not study perovskite hydrides that can only be stable above 50 GPa.

For dynamically stable ternary perovskite hydrides, we further determined their thermodynamic stability. We built a database for high pressure phase of elements and binary hydrides at 0-50 GPa. Ab initio random structure searches were performed in each AXH_3 compound at pressure of 0-50 GPa to supplement the enthalpy information of ternary compounds. Based on the database, a high-throughput code was developed to construct ternary convex hull

graphs. The enthalpy values deviating from the ternary convex hull line are shown as the color of markers in Fig. 2. The bluer the color means more thermodynamically stable. The circular marks indicates that these structures are metastable within 50 GPa, and the square marks indicates that these structures are thermodynamically stable. In this study, we have uncovered three thermodynamically stable perovskite hydrides, KGaH_3 , RbGaH_3 and CsInH_3 . It is worth noting that for the structure KInH_3 , which was previously mentioned to be stable at ambient pressure, we have conducted calculations with various accuracies. Finally, it was found that our calculation result with q-point of $3 \times 3 \times 3$ was in good agreement with previous work. But with q-point of $6 \times 6 \times 6$, KInH_3 cannot stabilize at ambient pressure (see Fig. S2 in Supplemental Material). In our calculations, KInH_3 can only dynamically stabilize at pressure above 20 GPa.

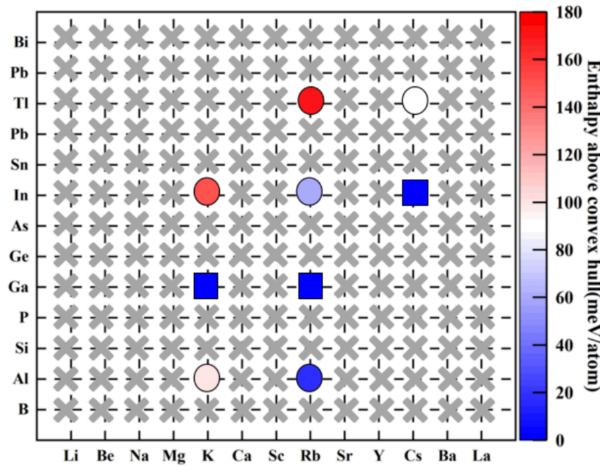


Fig. 2. The circular marks indicate the dynamically stable perovskite hydrides AXH_3 at 50 GPa. The square marks indicate the thermodynamically stable AXH_3 at pressure lower than 50 GPa. The gray cross represents the AXH_3 that are dynamically unstable at pressure lower than 50 GPa. The enthalpy values of AXH_3 above the convex hull are represented by the color of markers. The color bar indicates the correspondence between the color and values.

We calculated the electron-phonon coupling (EPC) to estimate the superconductivity. The T_{cS} are estimated through the self-consistent iteration solution of the Eliashberg equation (scE) with

$\mu^*=0.10$ as a function of pressure are supplied in Fig. 3. RbTiH₃ shows the highest T_c of 170 K at 4 GPa, followed by CsTiH₃ with T_c of 163 K at 7 GPa. But unfortunately, both of them are metastable phases, this means that some difficulties need to be overcome in the experiment to synthesize these structures. Considering the continuous progress in the synthesis technology of metastable materials in experiments, there is also a considerable possibility that we will see these excellent properties of metastable materials successfully synthesized in the future⁵⁰. CsInH₃ shows the highest T_c of 153 K at 9 GPa in all thermodynamically stable perovskite hydrides, followed by KGaH₃ with a T_c of 146 K at 10 GPa. RbGaH₃ requires more than 20 GPa to be dynamically stable, and its T_c is expected to be 127 K at this time. In addition, the metastable phase RbInH₃ also exhibits good properties, with a T_c of 130 K at 6 GPa. Other metastable phase KAlH₃ and RbAlH₃ shows the T_c of 95 K at 7 GPa and 86 K at 15 GPa respectively. Detailed computational results at different pressures are supplied in Table S1 in the Supplemental Material. In addition, the T_c s of these perovskite hydrides are more sensitive to pressure than other hydrides. RbTiH₃ shows the T_c of 170 K at 4 GPa, but as the pressure increased to 20 GPa, its T_c rapidly decreased to 81 K. The T_c of KGaH₃, CsInH₃, and CsTiH₃ also rapidly decrease with increasing pressure.

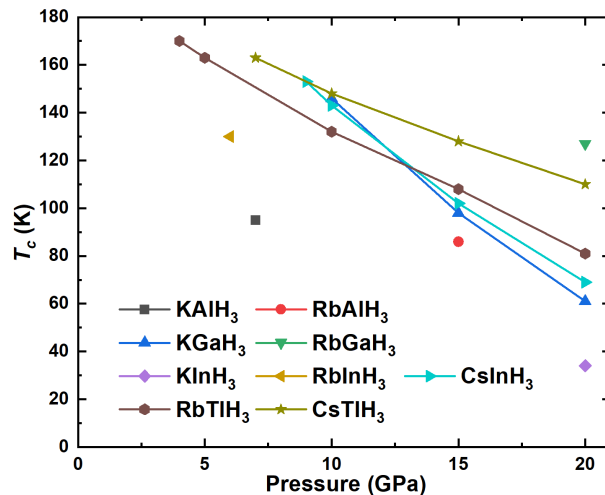


Fig. 3. The T_c s of perovskite hydrides AXH_3 estimated through the self-consistent iteration solution of the Eliashberg equation as a function of pressures.

We furthermore calculated the electron localization function (ELF) and Bader charge of these perovskite hydrides at different pressures (see Fig. 4). The structure of perovskite hydride AXH_3 can be divided into two parts: alkali metals, and the framework structure formed by IIIA group elements and hydrogen. Fig. 4a shows the ELF of the alkali metal layer of $RbAlH_3$, charge localization around alkali metal Rb. This indicates that the alkali metal Rb plays a "pre-compressor" role to support the framework structure formed by IIIA group elements and hydrogen in $RbAlH_3$ and does not directly contribute to superconductivity. The ELF of the alkali metal layer in other AXH_3 structures is basically consistent with Fig. 4a (see Fig. S3 in the Supplemental Material), which means that alkali metals play a "pre-compressor" role in all perovskite hydrides AXH_3 . From Fig. 4e, it can be seen that the electrons provided by the alkali metal Rb in $RbXH_3$ ($X = Al, Ga, In, Tl$) remain in a relatively stable range (0.69 e - 0.77 e). Even if replaced with other alkali metals with different radii, the electrons provided by alkali metals in $AInH_3$ ($A = K, Rb, Cs$) remain within a relatively stable range (0.71 e - 0.72 e). This means that alkali metals also act as electron donors in AXH_3 , and alkali metals provide a relatively fixed number of electrons. Changes in elements and pressure have little effect on the number of electrons provided by alkali metals.

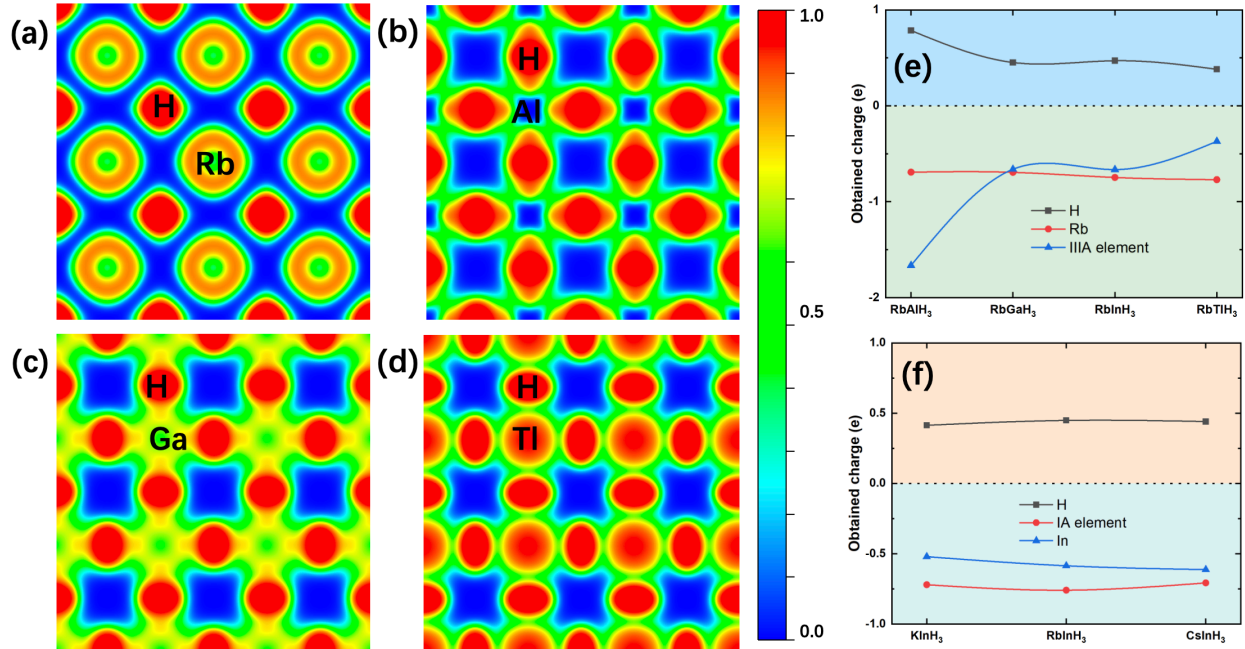


Fig. 4. The 2-dimensional electron localization function (ELF) for perovskite hydrides (a) RbAlH₃ at alkali metal layer, (b) RbAlH₃, (c) RbGaH₃ and (d) RbTIH₃ at IIIA group atomic layer. Remnant charges on A, X and H atoms obtained from Bader Charge Analysis of (e) RbXH₃ (X = Al, Ga, In, TI) and (f) AInH₃ (A = K, Rb, Cs).

Fig. 4b-d shows the ELF of the IIIA group atomic layers in RbAlH₃, RbGaH₃ and RbTIH₃, respectively. The IIIA group atomic layers in different AXH₃ exhibit significant differences, both in charge density and charge distribution. The Al layer in RbAlH₃ has the lowest charge density in RbXH₃ (X = Al, Ga, In, TI), and the charges around H are distributed in an ellipsoidal shape, with the ellipsoidal axis along the Al-H direction (see Fig. 4b). The Ga layer in RbGaH₃ has the highest charge density, and the charges around H are distributed in a spherical shape (see Fig. 4c), and the ELF of the In layer in RbInH₃ is also basically similar (see Fig. S3 in the Supplemental Material). The TI layer in RbTIH₃ has the moderate charge density, and the charges around H are distributed in an ellipsoidal shape, with the ellipsoidal axis perpendicular to the TI-H direction (see Fig. 4d). It can be seen that the X-H framework formed by IIIA group elements and

hydrogen is the key to the superconductivity of the AXH₃ system, and the charge density and distribution on the B-H framework will affect the superconductivity of the system. From Fig. 4e, it can also be seen that there are significant differences in charge transfer between different IIIA group elements, with Al transferring up to 1.66 e of charge, while Tl only transferring 0.37 e of charge. Considering the superconductivity and stability of each AXH₃ in Fig.2-3, we believe that the Tl element with the least charge transfer (0.37 e) is more conducive to high-temperature superconductivity and low-pressure dynamic stability of the structure, while the Ga and In elements with moderate charge transfer (0.66 e) are more conducive to thermodynamic stability of the structure.

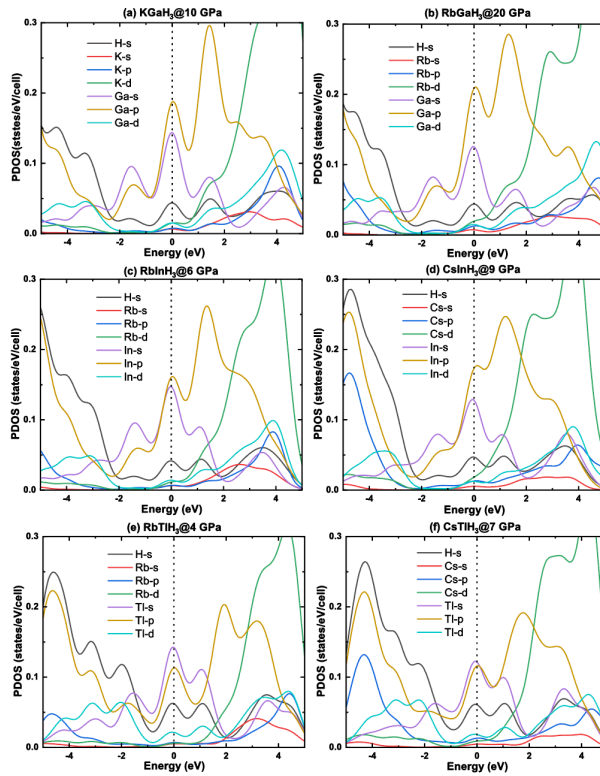


Fig. 5. The projected electronic density of states of (a) KGaH₃ at 10 GPa, (b) RbGaH₃ at 20 GPa, (c) RbInH₃ at 6 GPa, (d) CsInH₃ at 9 GPa, (e) RbTlH₃ at 4 GPa and (f) CsTlH₃ at 7 GPa.

Subsequently, we calculated the electronic band structures (see Fig. S4 in the Supplemental Material) and projected density of states (PDOS) to understand the effect of pressure on the electronic structure for KGaH_3 at 10 GPa, RbGaH_3 at 20 GPa, RbInH_3 at 3 GPa, CsInH_3 at 9 GPa, RbTIH_3 at 4 GPa and CsTIH_3 at 7 GPa. As shown in Fig. 5, AXH_3 share the similar electronic structure with peak of DOS located above the Fermi energy level (E_f), contributions from s-orbitals and p-orbitals in IIIA element dominate the DOS at the Fermi level. When the IIIA elements are the same, the electronic structure of AXH_3 is basically the same, which is also consistent with the results in Fig. 4f. The key difference in electronic structure of AXH_3 lies in the contribution of hydrogen on the Fermi surface. The contribution of H in the Fermi surface is higher in RbTIH_3 and CsTIH_3 , which may be an important reason for their higher T_c . Based on the charge transfer situation in Fig. 4e, we believe that in AXH_3 , less charge transfer is more favorable for the DOS peak of hydrogen near the Fermi surface, leading to a higher superconducting transition temperature. The X-H covalent framework is the key to AXH_3 high-temperature superconductivity. As hydrogen gains too many electrons and exhibits hydrogen ion properties, its DOS will appear more in deep energy levels rather than near the Fermi surface.

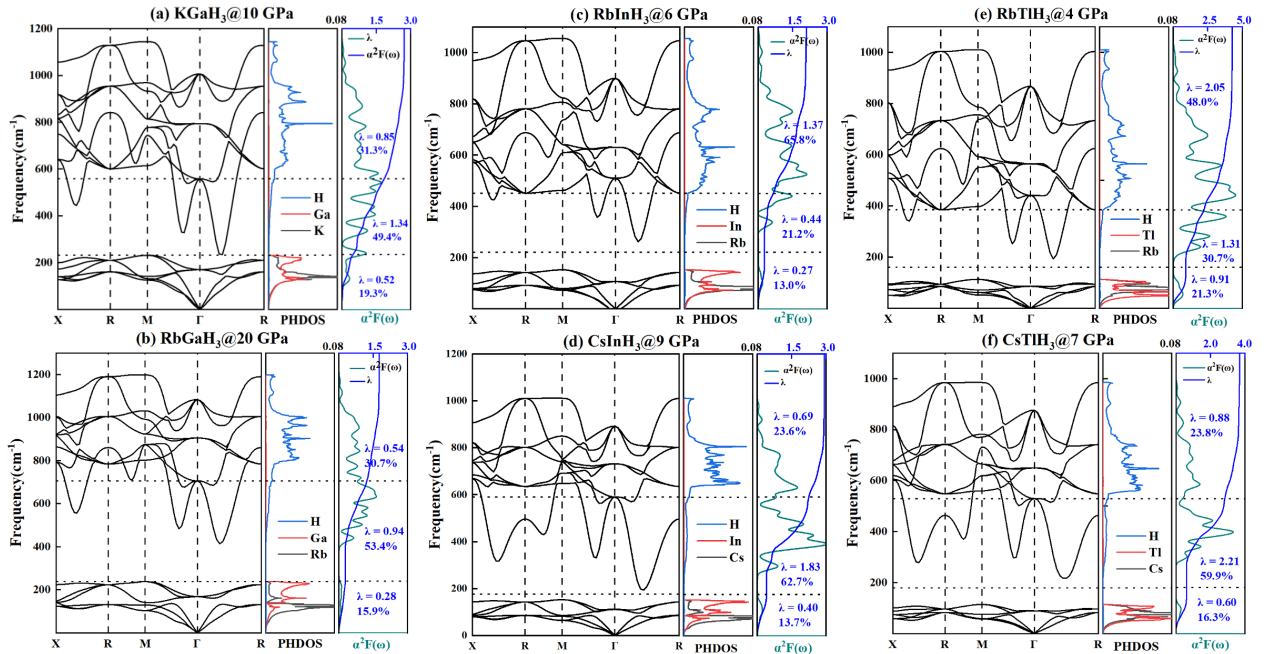


Fig. 6. Calculated phonon dispersion curves, phonon density of states (PHDOS), Eliashberg spectral function $\alpha^2F(\omega)$ and the accumulated EPC constant λ of (a) KGaH_3 at 10 GPa, (b)

RbGaH₃ at 20 GPa, (c) RbInH₃ at 6 GPa, (d) CsInH₃ at 9 GPa, (e) RbTIH₃ at 4 GPa and (f) CsTIH₃ at 7 GPa.

To further understand the source of high temperature superconductivity of these perovskite hydrides AXH₃, we calculated the phonon band structure, projected phonon density of states (PHDOS), accumulated electron-phonon coupling (EPC) parameter λ , and Eliashberg spectral function $\alpha^2F(\omega)$ of KGaH₃ at 10 GPa, RbGaH₃ at 20 GPa, RbInH₃ at 3 GPa, CsInH₃ at 9 GPa, RbTIH₃ at 4 GPa and CsTIH₃ at 7 GPa, as shown in Fig. 6. It can be seen from PHDOS that the low frequency phonon modes (below 200 cm⁻¹) are mainly from IA and IIIA elements, high frequency phonon modes (above 200 cm⁻¹) are mainly from H atom. The accumulated EPC constant λ in the low-frequency region accounts for 13% - 21.3% of the total λ , indicating that non-hydrogen elements contribute less to the electron-phonon coupling. The key of these perovskite hydrides AXH₃ to high-temperature superconductivity, like other hydrides, is also related to the high-frequency vibration of hydrogen.

As we discussed in Fig. 3, the T_c s of these perovskite hydrides are more sensitive to pressure than other hydrides. From the phonon band structure, it is likely due to a significant contribution of phonon softening in the superconductivity of these structures. The accumulated EPC constant λ in the phonon softening region accounts for 21.2 % - 62.7% of the total λ , which is higher than the contribution of non-hydrogen elements. Furthermore, it should be noted that a considerable portion of the electroacoustic coupling in the high-frequency region also comes from phonon softening, such as phonon softening near the frequency of 600 cm⁻¹ on the high symmetry path X-R-M in RbInH₃ and RbTIH₃ (see Fig. 6c and 6e). And The growth of accumulated EPC constant λ is most rapid around the frequency around 600 cm⁻¹. Considering this, we can consider that phonon softening contributes more than 50% to the electron-phonon coupling

among the six perovskite hydrides AXH_3 in Fig. 6. When the pressure increases, phonon softening weakens, and the corresponding electron-phonon coupling rapidly weakens, ultimately leading to the rapid decrease in T_c . The calculated EPC constant λ , logarithmic average phonon frequency ω_{\log} , superconducting critical temperature T_c for perovskite hydrides AXH_3 at different pressures are list in Table. S3 in the Supplemental Material. It can be clearly seen that as the pressure increases to 20 GPa, the λ of $CsInH_3$ rapidly decreases from 2.92 to 1.24, and T_c of $CsInH_3$ decreases from 153 K to 69 K; the λ of $RbTIH_3$ decreases from 4.27 to 1.28, and T_c of $RbTIH_3$ decreases from 170 K to 81 K; the λ of $CsTIH_3$ decreases from 3.69 to 1.48, and T_c of $RbTIH_3$ decreases from 163 K to 110 K. This high sensitivity of T_c to pressure may result in higher requirements for precise pressure control in future experimental synthesis of such hydrides. But from another perspective, this sensitivity may allow them to be applied in more fields beyond high-temperature superconductivity.

Conclusions

In summary, we have designed a series of high-temperature superconductors that can be stable within 10 GPa based on perovskite structure of $Pm-3m-KInH_3$. Our research covered 182 ternary systems and ultimately determined that 9 compounds were stable within 20 GPa, of which 5 exhibited superconducting transition temperatures exceeding 120 K within 10 GPa, including $KGaH_3$ (146 K at 10 GPa), $RbInH_3$ (130 K at 6 GPa), $CsInH_3$ (153 K at 9 GPa), $RbTIH_3$ (170 K at 4 GPa) and $CsTIH_3$ (163 K at 7 GPa). Excitingly, $KGaH_3$ and $CsInH_3$ are thermodynamically stable at 50 GPa. Among these perovskite hydrides, alkali metals are responsible for providing a fixed amount of charge and maintaining structural stability, while the cubic framework formed by IIIA group elements and hydrogen is crucial for high-temperature superconductivity. EPC calculations revealed that the contribution of the softening phonon mode

of hydrogen to the EPC constant λ exceeds 50%. This phonon softening enables these hydrides to exhibit unexpectedly high superconducting transition temperatures at low pressures, but as the pressure increases, the softening decreases, and their superconducting transition temperature rapidly decreases to less than half of its maximum T_c . This high sensitivity of T_c to pressure may result in higher requirements for precise pressure control in future experimental synthesis of such hydrides. But from another perspective, this sensitivity may allow them to be applied in more fields beyond high-temperature superconductivity. This work will inspire further experimental exploration and take an important step in the exploration of low-pressure stable high-temperature superconductors.

REFERENCES

- ¹E. Wigner, H.B. Huntington, "On the Possibility of a Metallic Modification of Hydrogen," J. Chem. Phys. 3, 764-770 (1935).
- ²J. Bardeen, L.N. Cooper, J.R. Schrieffer, "Microscopic Theory of Superconductivity," Phys. Rev. 106, 162-164 (1957).
- ³N.W. Ashcroft, "Metallic Hydrogen: A High-Temperature Superconductor?," Phys. Rev. Lett. 21, 1748 (1968).
- ⁴R.P. Dias, I.F. Silvera, "Observation of the Wigner-Huntington transition to metallic hydrogen," Science 355, 715-718 (2017).
- ⁵P. Loubeyre, F. Occelli, P. Dumas, "Synchrotron infrared spectroscopic evidence of the probable transition to metal hydrogen," Nature 577, 631 (2020).
- ⁶N.W. Ashcroft, "Hydrogen dominant metallic alloys: High temperature superconductors?," Phys. Rev. Lett. 92, 4 (2004).
- ⁷D.F. Duan, Y.X. Liu, Y.B. Ma, Z. Shao, B.B. Liu, T. Cui, "Structure and superconductivity of hydrides at high pressures," Natl. Sci. Rev. 4, 121-135 (2017).
- ⁸L.P. Gorkov, V.Z. Kresin, "Colloquium: High pressure and road to room temperature superconductivity," Rev. Mod. Phys. 90, 16 (2018).
- ⁹M. Du, W. Zhao, T. Cui, D. Duan, "Compressed superhydrides: the road to room temperature superconductivity," Journal of Physics: Condensed Matter 34, 173001 (2022).
- ¹⁰D.F. Duan, Y.X. Liu, F.B. Tian, D. Li, X.L. Huang, Z.L. Zhao, H.Y. Yu, B.B. Liu, W.J. Tian, T. Cui, "Pressure-induced metallization of dense (H₂S)₍₂₎H-2 with high-T_c superconductivity," Sci Rep 4, 6 (2014).
- ¹¹H.Y. Liu, Naumov, II, R. Hoffmann, N.W. Ashcroft, R.J. Hemley, "Potential high-T_c superconducting lanthanum and yttrium hydrides at high pressure," Proc. Natl. Acad. Sci. U. S. A. 114, 6990-6995 (2017).

- ¹²F. Peng, Y. Sun, C.J. Pickard, R.J. Needs, Q. Wu, Y.M. Ma, "Hydrogen Clathrate Structures in Rare Earth Hydrides at High Pressures: Possible Route to Room-Temperature Superconductivity," *Phys. Rev. Lett.* 119, 6 (2017).
- ¹³A.P. Drozdov, M.I. Eremets, I.A. Troyan, V. Ksenofontov, S.I. Shylin, "Conventional superconductivity at 203 kelvin at high pressures in the sulfur hydride system," *Nature* 525, 73 (2015).
- ¹⁴M. Einaga, M. Sakata, T. Ishikawa, K. Shimizu, M.I. Eremets, A.P. Drozdov, I.A. Troyan, N. Hirao, Y. Ohishi, "Crystal structure of the superconducting phase of sulfur hydride," *Nat. Phys.* 12, 835–838 (2016).
- ¹⁵A.P. Drozdov, P.P. Kong, V.S. Minkov, S.P. Besedin, M.A. Kuzovnikov, S. Mozaffari, L. Balicas, F.F. Balakirev, D.E. Graf, V.B. Prakapenka, E. Greenberg, D.A. Knyazev, M. Tkacz, M.I. Eremets, "Superconductivity at 250 K in lanthanum hydride under high pressures," *Nature* 569, 528 (2019).
- ¹⁶M. Somayazulu, M. Ahart, A.K. Mishra, Z.M. Geballe, M. Baldini, Y. Meng, V.V. Struzhkin, R.J. Hemley, "Evidence for Superconductivity above 260 K in Lanthanum Superhydride at Megabar Pressures," *Phys. Rev. Lett.* 122, 6 (2019).
- ¹⁷H. Wang, J.S. Tse, K. Tanaka, T. Iitaka, Y. Ma, "Superconductive sodalite-like clathrate calcium hydride at high pressures," *Proc. Natl. Acad. Sci. U. S. A.* 109, 6463 (2012).
- ¹⁸X. Feng, J. Zhang, G. Gao, H. Liu, H. Wang, "Compressed sodalite-like MgH₆ as a potential high-temperature superconductor," *RSC Adv.* 5, 59292–59296 (2015).
- ¹⁹Y. Li, J. Hao, H. Liu, J.S. Tse, Y. Wang, Y. Ma, "Pressure-stabilized superconductive yttrium hydrides," *Sci Rep* 5, 9948 (2015).
- ²⁰K. Abe, "Hydrogen-rich scandium compounds at high pressures," *Phys. Rev. B* 96, 144108 (2017).
- ²¹Hao Song, Zihan Zhang, Tian Cui, Chris J. Pickard, Vladimir Z. Kresin, D. Duan, "High Tc Superconductivity in Heavy Rare Earth Hydrides," *Chinese Physics Letters* 38, 107401 (2021).
- ²²H. Xie, D.F. Duan, Z.J. Shao, H. Song, Y.C. Wang, X.H. Xiao, D. Li, F.B. Tian, B.B. Liu, T. Cui, "High-temperature superconductivity in ternary clathrate YCaH₁₂ under high pressures," *J. Phys.-Condes. Matter* 31, 7 (2019).
- ²³X. Liang, A. Bergara, L. Wang, B. Wen, Z. Zhao, X.-F. Zhou, J. He, G. Gao, Y. Tian, "Potential high-Tc superconductivity in CaYH₁₂ under pressure," *Phys. Rev. B* 99, 100505 (2019).
- ²⁴W. Zhao, D. Duan, M. Du, X. Yao, Z. Huo, Q. Jiang, T. Cui, "Pressure-induced high-Tc superconductivity in the ternary clathrate system Y-Ca-H," *Phys. Rev. B* 106, 014521 (2022).
- ²⁵W. Sukmas, P. Tsuppayakorn-aek, U. Pinsook, T. Bovornratanaraks, "Near-room-temperature superconductivity of Mg/Ca substituted metal hexahydride under pressure," *J. Alloy. Compd.* 849, 156434 (2020).
- ²⁶L.-T. Shi, Y.-K. Wei, A.K. Liang, R. Turnbull, C. Cheng, X.-R. Chen, G.-F. Ji, "Prediction of pressure-induced superconductivity in the novel ternary system ScCaH_{2n} (n = 1–6)," *Journal of Materials Chemistry C* 9, 7284–7291 (2021).
- ²⁷P. Song, Z. Hou, P.B.d. Castro, K. Nakano, K. Hongo, Y. Takano, R. Maezono, "High-Tc Superconducting Hydrides Formed by LaH₂₄ and YH₂₄ Cage Structures as Basic Blocks," *Chem. Mat.* 33, 9501–9507 (2021).
- ²⁸M. Du, H. Song, Z. Zhang, D. Duan, T. Cui, "Room-Temperature Superconductivity in Yb/Lu Substituted Clathrate Hexahydrides under Moderate Pressure," *Research* 2022, 9784309 (2022).
- ²⁹D.V. Semenov, A.G. Kvashnin, A.G. Ivanova, V. Svitlyk, V.Y. Fomin, A.V. Sadakov, O.A. Sobolevskiy, V.M. Pudalov, I.A. Troyan, A.R. Oganov, "Superconductivity at 161 K in thorium hydride ThH₁₀: Synthesis and properties," *Mater. Today* 33, 36–44 (2020).

- ³⁰P. Kong, V.S. Minkov, M.A. Kuzovnikov, A.P. Drozdov, S.P. Besedin, S. Mozaffari, L. Balicas, F.F. Balakirev, V.B. Prakapenka, S. Chariton, D.A. Knyazev, E. Greenberg, M.I. Eremets, "Superconductivity up to 243 K in the yttrium–hydrogen system under high pressure," *Nat. Commun.* 12, 5075 (2021).
- ³¹E. Snider, N. Dasenbrock–Gammon, R. McBride, X. Wang, N. Meyers, K.V. Lawler, E. Zurek, A. Salamat, R.P. Dias, "Synthesis of Yttrium Superhydride Superconductor with a Transition Temperature up to 262 K by Catalytic Hydrogenation at High Pressures," *Phys. Rev. Lett.* 126, 117003 (2021).
- ³²Y. Wang, K. Wang, Y. Sun, L. Ma, Y. Wang, B. Zou, G. Liu, M. Zhou, H. Wang, "Synthesis and superconductivity in yttrium superhydrides under high pressure," *Chinese Physics B* (2022).
- ³³L. Ma, K. Wang, Y. Xie, X. Yang, Y. Wang, M. Zhou, H. Liu, X. Yu, Y. Zhao, H. Wang, G. Liu, Y. Ma, "High–Temperature Superconducting Phase in Clathrate Calcium Hydride CaH₆ up to 215 K at a Pressure of 172 GPa," *Phys. Rev. Lett.* 128, 167001 (2022).
- ³⁴Z. Li, X. He, C. Zhang, X. Wang, S. Zhang, Y. Jia, S. Feng, K. Lu, J. Zhao, J. Zhang, B. Min, Y. Long, R. Yu, L. Wang, M. Ye, Z. Zhang, V. Prakapenka, S. Chariton, P.A. Ginsberg, J. Bass, S. Yuan, H. Liu, C. Jin, "Superconductivity above 200 K discovered in superhydrides of calcium," *Nat. Commun.* 13, 2863 (2022).
- ³⁵I.A. Troyan, D.V. Semenov, A.G. Kvashnin, A.V. Sadakov, O.A. Sobolevskiy, V.M. Pudalov, A.G. Ivanova, V.B. Prakapenka, E. Greenberg, A.G. Gavriliuk, I.S. Lyubutin, V.V. Struzhkin, A. Bergara, I. Errea, R. Bianco, M. Calandra, F. Mauri, L. Monacelli, R. Akashi, A.R. Oganov, "Anomalous High–Temperature Superconductivity in YH₆," *Adv. Mater.* 33, 2006832 (2021).
- ³⁶W. Chen, D.V. Semenov, X. Huang, H. Shu, X. Li, D. Duan, T. Cui, A.R. Oganov, "High–Temperature Superconducting Phases in Cerium Superhydride with a T_c up to 115 K below a Pressure of 1 Megabar," *Phys. Rev. Lett.* 127, 117001 (2021).
- ³⁷D.V. Semenov, I.A. Troyan, A.G. Ivanova, A.G. Kvashnin, I.A. Kruglov, M. Hanfland, A.V. Sadakov, O.A. Sobolevskiy, K.S. Pervakov, I.S. Lyubutin, K.V. Glazyrin, N. Giordano, D.N. Karimov, A.L. Vasiliev, R. Akashi, V.M. Pudalov, A.R. Oganov, "Superconductivity at 253 K in lanthanum–yttrium ternary hydrides," *Mater. Today* 48, 18–28 (2021).
- ³⁸W. Chen, X. Huang, D.V. Semenov, S. Chen, K. Zhang, A.R. Oganov, T. Cui, Enhancement of the superconducting critical temperature realized in the La–Ce–H system at moderate pressures, 2022, pp. arXiv:2203.14353.
- ³⁹J. K. Bi, Y. Nakamoto, P.Y. Zhang, K. Shimizu, B. Zou, H.Y. Liu, M. Zhou, G.T. Liu, H.B. Wang, Y.M. Ma, "Giant enhancement of superconducting critical temperature in substitutional alloy (La,Ce)₂H–9," *Nat. Commun.* 13 (2022).
- ⁴⁰T.F.T. Cerqueira, Y.–W. Fang, I. Errea, A. Sanna, M.A.L. Marques, "Searching Materials Space for Hydride Superconductors at Ambient Pressure," *Advanced Functional Materials* n/a, 2404043 (2024).
- ⁴¹C.J. Pickard, R.J. Needs, "High–pressure phases of silane," *Phys. Rev. Lett.* 97, 4 (2006).
- ⁴²C.J. Pickard, R.J. Needs, "Ab initio random structure searching," *J. Phys.–Condes. Matter* 23, 23 (2011).
- ⁴³S.J. Clark, M.D. Segall, C.J. Pickard, P.J. Hasnip, M.J. Probert, K. Refson, M.C. Payne, "First principles methods using CASTEP," *Z. Kristall.* 220, 567–570 (2005).
- ⁴⁴J.P. Perdew, K. Burke, M. Ernzerhof, "Generalized Gradient Approximation Made Simple," *Phys. Rev. Lett.* 77, 3865 (1996).
- ⁴⁵Kresse, Furthmuller, "Efficient iterative schemes for ab initio total–energy calculations using a plane–wave basis set," *Phys. Rev. B* 54, 11169–11186 (1996).
- ⁴⁶G. Kresse, D. Joubert, "From ultrasoft pseudopotentials to the projector augmented–wave method," *Phys. Rev. B* 59, 1758–1775 (1999).

⁴⁷D. J. Chadi, "Special points for Brillouin-zone integrations," *Phys. Rev. B* 16, 1746 (1977).

⁴⁸P. Giannozzi, S. Baroni, N. Bonini, M. Calandra, R. Car, C. Cavazzoni, D. Ceresoli, G.L. Chiarotti, M. Cococcioni, I. Dabo, A. Dal Corso, S. de Gironcoli, S. Fabris, G. Fratesi, R. Gebauer, U. Gerstmann, C. Gougoussis, A. Kokalj, M. Lazzeri, L. Martin-Samos, N. Marzari, F. Mauri, R. Mazzarello, S. Paolini, A. Pasquarello, L. Paulatto, C. Sbraccia, S. Scandolo, G. Sclauzero, A.P. Seitsonen, A. Smogunov, P. Umari, R.M. Wentzcovitch, "QUANTUM ESPRESSO: a modular and open-source software project for quantum simulations of materials," *J. Phys.-Condes. Matter* 21, 19 (2009).

⁴⁹G. M. Eliashberg, "Interactions between electrons and lattice vibrations in a superconductor," *Sov Phys Jetp* 11:3, 696-702 (1960).

⁵⁰J. A. Flores-Livas, A. Sanna, A. P. Drozdov, L. Boeri, G. Profeta, M. Eremets, S. Goedecker, "Interplay between structure and superconductivity: Metastable phases of phosphorus under pressure," *Physical Review Materials* 1, 024802 (2017).